Relative Nucleophilicity: The Role of Solvation and Thermodynamics

Robert D. Bach,*,† Julia E. Winter,† and Joseph J. W. McDouall‡

Contribution from the Departments of Chemistry, Wayne State University, Detroit, Michigan 48202, and University of Manchester, Manchester M13 9PL, United Kingdom

Received January 11, 1995. Revised Manuscript Received June 9, 1995[⊗]

Abstract: The relative reactivity of a series of nucleophiles that includes alkenes, sulfides, sulfoxides, amines, and phosphines toward peroxyformic acid has been examined at an *ab initio* level of theory MP4SDTQ//MP2/6-31G*. Solvation effects and the exo- versus endothermicity of oxygen transfer from a peroxy acid (:NUC + HCO_3H → O−NUC + HCO_2H) has a much greater influence upon the relative nucleophilicity than polarizability. The intrinsic reactivity of dimethyl sulfide was found to be nearly identical to that of dimethyl sulfoxide. The classical gas phase barrier for oxidation of trimethylamine to trimethylamine oxide was also only slightly higher (0.4 kcal/mol) than that for oxygen atom transfer to trimethylphosphine. When the transition states were examined by self-consistent reaction field (SCRF) methods the predicted barriers were found to be in good agreement with experiment. Protic solvents are shown to play a major role in determining the relative reactivity of this series of nucleophiles.

Introduction

Chemical descriptors such as electrophiles and nucleophiles have been used advantageously to define chemical reactivity factors. More recently efforts have been directed toward separating intrinsic reactivity parameters in the gas phase from those that can be attributed to solvent effects in the condensed phase. Consequently the distinction between those reagents that are classified as either electrophilic or nucleophilic has become more difficult to define. Relative nucleophilic character is typically assigned to those reagents that donate readily an electron pair to a reagent that has been deemed electrophilic in nature. When one nucleophile is considered to be more reactive than another, the relative reactivity is typically that measured in solution. Among those properties that influence nucleophilicity are the degree of solvation of the nucleophile, its effective size and electronegativity, and the polarizability of the attacking atom. For example, third-row elements are considered to be more nucleophilic than the second-row counterparts and this increased nucleophilicity is often ascribed to their greater polarizability.[1]

Historically, peroxy acids, hydroperoxides, and protonated hydroperoxides have been deemed electrophilic in nature. In fact, early investigators suggested that oxidation reactions involving oxygen atom transfer from the −OOH moiety operated mechanistically as sources of hydroxyl cation (HO^+) that reacted with a nucleophilic species.[2] Current theoretical studies suggest that the net nuclear event involved kinetically in oxidation reactions with the −OOH functionality is indeed the formal transfer of HO^+ albeit in concert with rate-limiting O−O bond cleavage.[3] Since heterolytic O−O bond breaking is involved with each of these reagents, the lowest activation pathway for oxidation reactions must involve a proton transfer or proton relay that helps to minimize charge separation. For example, oxygen atom transfer from an alkyl hydrogen peroxide (RO−OH) involves a proton transfer from ROOH or a protic solvent to produce a neutral leaving group (ROH).[4] A peroxy acid (RCO_3H) is a particularly efficient oxygen atom donor because a 1,4-intramolecular hydrogen transfer affords a neutral leaving group (RCO_2H) that greatly diminishes obligatory charge separation along the reaction coordinate.[5] As a consequence, peroxy acids are typically 10^3 more reactive than alkyl hydroperoxides.[6] We prefer to define an electrophile that does not bear a positive charge as a reagent possessing a relatively weak σ-bond that readily experiences bond elongation upon attack by a nucleophile with an attendant formation of an empty (electrophilic) σ^* orbital.[5,7] In this report we examine the relative reactivity of a series of nucleophiles toward a common electrophile, peroxyformic acid, in both the condensed and gas phase. For the relative reactivity of the former phase we resort to the experimental literature and for the latter we use *ab initio* molecular orbital theory.

Method of Calculation

Molecular orbital calculations were carried out using the Gaussian 92 program system[8a] utilizing gradient geometry optimization.[8b] The geometries of HCO_3H, nucleophiles (H_2S, NH_3, C_2H_4, PH_3, $(CH_3)_2S$, $(CH_3)_2SO$, $(CH_3)_3N$, and $(CH_3)_3P$), and the transition structures were first determined at the MP2/3-21G level of theory. All geometries were then fully optimized without geometry constraints using second-order Møller−Plesset perturbation theory (full MP2/6-31G*). Relevant

† Wayne State University.

‡ University of Manchester.

[⊗] Abstract published in *Advance ACS Abstracts,* August 1, 1995.

(1) (a) Carey, F. A.; Sundberg, R. J. *Advanced Organic Chemistry*, 3rd ed.; Plenum Press: New York, 1990; Part A, p 284. (b) Lowry, T. H.; Richardson, K. S. *Mechanism and Theory in Organic Chemistry*, 3rd ed.; Harper & Row: New York, 1987; p 367.

(2) Waters, W. A. *Mechanism of Oxidation of Organic Compounds*; John Wiley & Sons: New York, 1965.

(3) (a) Bach, R. D.; Su, M.-D.; Schlegel, H. B. *J. Am. Chem. Soc.* **1994**, *116*, 5379. (b) Bach, R. D.; Su, M.-D. *J. Am. Chem. Soc.* **1994**, *116*, 5392.

(4) (a) For a discussion of solvent assisted proton transfer in alkyl hydrogen peroxides see: Dankleff, M. A. P.; Ruggero, C.; Edwards, J. O.; Pyun, H. Y. *J. Am. Chem. Soc.* **1968**, *90*, 3209. (b) Curci, R.; DiPrete, R. A.; Edwards, J. O.; Modena, G. *J. Org. Chem.* **1970**, *35*, 740. (c) Curci, R.; Edwards, J. O. In *Catalytic Oxidations with H_2O_2 as Oxidants*; Strukul, G., Ed.; Series: Catalysis by Metal Complexes; Reidel-Kluwer: Dordrecht, The Netherlands, 1992; Chapter 3. (d) Curci, R. *Advances in Oxygenated Processes*; Baumstark, A. L., Ed.; JAI Press: Greenwich, CT, **1990**; Vol. 2, Chapter 1, pp 1−59. (e) DiFuria, F.; Modena, G. *Pure Appl. Chem.* **1982**, *54*, 1853.

(5) Bach, R. D.; Owensby, A.; Gonzalez, C.; Schlegel, H. B. *J. Am. Chem. Soc.* **1991**, *113*, 2238.

(6) Plesnicar, B. *The Chemistry of Functional Groups*; Patai, S., Ed.; John Wiley: New York, 1983; p 521.

(7) (a) Bach, R. D.; Andres, J. L.; Davis, F. A. *J. Org. Chem.* **1992**, *57*, 613. (b) Bach, R. D.; Coddens, B. A.; McDouall, J. J. W.; Schlegel, H. B.; Davis, F. A. *J. Org. Chem.* **1990**, *55*, 3325.

0002-7863/95/1517-8586$09.00/0

Table 1. Total Energies for Peroxyformic Acid Transition States, Reactant Clusters, Reactants, and Products (Energies in hartrees)

	MP2/3-21G	MP2/3-21G ZPE correction	MP2/6-31G*	MP2/6-31G* [a] ZPE correction	MP4/6-31G*//MP2/6-31G*	PMP4/6-31G*// [b] MP2/6-31G*	stability test root
1 (C_2H_4)			−342.488 97	0.090 94	−342.540 54		
TS-2			−342.455 88	0.091 16	−342.508 28	−342.504 12	−0.110
3 (H_2S)			−662.992 66	0.055 07	−663.032 11		
TS-4			−662.946 88	0.055 02	−662.089 44	−662.989 86	−0.006
5 (H_2SO)			−737.961 29	0.060 94	−738.002 94		
TS-6			−737.927 76	0.061 56	−737.964 63	−737.971 79	−0.099
7 (Me_2S)	−737.134 50	0.115 81	−741.338 45		−741.398 14		
TS-8	−737.093 17	0.113 95	−741.316 41		−741.378 92		−0.045
9a (Me_2SO)	−811.593 84	0.117 93	−816.331 19				
9b		0.128 60 [d]	−816.339 58		−816.401 60		
TS-10	−811.551 37	0.116 91	−816.311 50		−816.376 42		−0.087
11 (NH_3)			−320.562 18	0.075 53	−320.601 76		
TS-12			−320.510 98	0.076 11	−320.556 43		stable
13 (PH_3)			−606.756 34	0.064 12	−606.798 52		
TS-14			−606.735 18	0.063 74	−606.777 63	−606.775 76	−0.081
15 (NMe_3)	−435.250 04	0.161 30	−438.054 57		−438.127 26		
TS-16	−435.222 18	0.161 53	−438.027 51		−438.106 52		−0.035
17 (PMe_3)	−720.080 74	0.153 49	−724.255 13		−724.366 13		
TS-18	−720.068 25	0.152 84	−724.242 83		−724.354 10		−0.081
reactants and products							
HCO_3H	−262.520 21	0.037 49	−264.187 82	0.037 54	−264.214 41		
C_2H_4			−78.294 29	0.052 08	−78.319 80		
H_2SO			−398.798 70	0.015 71	−398.812 00		
H_2SO			−473.761 30	0.021 80	−473.777 06		
Me_2S	−474.600 90	0.077 84	−477.141 32		−477.174 99		
Me_2SO	−549.061 40	0.080 37	−552.136 17		−552.172 34		
NH_3			−56.357 38	0.035 31	−56.371 26		
PH_3			−342.562 26	0.025 07	−342.578 31		
Me_3N	−172.700 59	0.124 09	−173.846 46		−173.893 61		
Me_3P	−457.546 06	0.116 10	−460.094 83		−460.140 55		
HCO_2H			−189.251 87		−189.270 63		
C_2H_4 epox			−153.315 69		−153.341 44		
H_2SO_2			−548.793 88		−548.806 30		
Me_2SO_2			−627.182 28		−627.216 00		
NH_3O					−131.302 67		
PH_3O			−417.609 65		−417.622 70		
Me_3NO			−248.778 70		−248.832 48		
Me_3PO			−535.180 51		−535.224 00		

[a] All MP2 geometries use the full 6-31G* basis set, except for reactant cluster **17** and **TS-18** which use the frozen core basis set. The MP2/6-31G* (frozen core) and MP4//MP2/6-31G* energies for peroxyformic acid and trimethylphosphine are −264.175 17, −264.214 46, −460.068 70, and −460.140 63, respectively. The MP2/6-31G* (frozen core) energies for formic acid and trimethylphosphine oxide are −189.241 78 and −535.150 42, respectively. [b] The projected MP4 energy reflects the total energy with spins $s + 1$ to $s + 4$ annihilated. [c] UHF stability test on the MP2/6-31G* transition state geometry. [d] The zero-point energy for reactant cluster **9b** is from the HF/6-31G* frequency calculation.

energies and barrier heights are then computed using the above geometry with fourth-order Møller−Plesset perturbation theory. This level is designated MP4SDTQ/6-31G*//MP2/6-31G*. Vibrational frequency calculations at the MP2/6-31G* level were used to characterize all stationary points bearing hydrogen substituents as either minima (zero imaginary frequencies) or first-order transition states (a single imaginary frequency). Frequency calculations on the methyl-substituted nucleophiles have been carried out for the MP2/3-21G optimized geometries. Total energies are given in Table 1.

The effects of solvation were obtained at the MP2 level, using gas-phase MP2/6-31G* geometries, for the Onsager[9] and Tomasi models.[10a] The self-consistent reaction field (SCRF) stabilization (relative to gas-phase) was obtained for reactants and transition states, and from this the overall stabilization of the barrier was calculated. One should accept the calculated barriers in solution as approximate but useful indicators of energetic trends. Relative energies are given in Table 2. Total energies for the SCRF calculations and the electron structures of the reactants and products are available as supporting information.

Results and Discussion

The level of theory that is required to describe adequately the ground state scission of the oxygen−oxygen bond in hydroperoxides has been the subject of considerable debate.[11] Fortunately, we have found that treatment of dynamic correlation at the MP2 level of theory is adequate for most geometries and several complete active space SCF (CASSCF) calculations have suggested that static correlation corrections are not as important as had been thought initially for O−O bond cleavage.[12] Historically, part of the difficulty in treating reaction potential

(8) (a) *GAUSSIAN 92*; Frisch, M. J.; Trucks, G. W.; Head-Gordon, M.; Gill, P. M. W.; Wong, M. W.; Foresman, J. B.; Johnson, B. G.; Schlegel, H. B.; Robb, M. A.; Replogle, E. S.; Gomperts, R.; Andres, J. L.; Raghavachari, K.; Binkley, J. S.; Gonzalez, C.; Martin, R. L.; Fox, D. J.; DeFrees, D. J.; Baker, J.; Stewart, J. J. P.; Pople, J. A.; Gaussian, Inc.: Pittsburgh, PA, **1992**. (b) Gonzalez, C.; Schlegel, H. B. *J. Chem. Phys.* **1989**, *90*, 2154.

(9) (a) Onsager, L. *J. Am. Chem. Soc.* **1936**, *58*, 1486. (b) Wong, M. W.; Frisch, M. J.; Wiberg, K. B. *J. Am. Chem. Soc.* **1991**, *113*, 4776.

(10) (a) Miertus, S.; Scrocco, E.; Tomasi, J. *J. Chem. Phys.* **1981**, *55*, 117. (b) Aguilar, M. A.; Olivares del Valle, F. J. O. *Chem. Phys.* **1989**, *129*, 439. (c) Rivail, J. L.; Terryn, B. *J. Chim. Phys., Phys.-Chem. Biol.* **1982**, *79*, 2. (d) Rinaldi, D. *Comput. Chem.* **1982**, *6*, 155. (e) Rinaldi, D.; Rivail, J. L.; Rguini, N. *J. Comput. Chem.* **1992**, *13*, 675.

(11) (a) Cremer, D. *The Chemistry of Peroxides*; Patai, S., Ed.; Wiley Interscience: New York, 1983; Chapter 1. (b) Richardson, W. H., ref 11a, Chapter 5.

(12) (a) Bach, R. D.; Owensby, A. L.; Gonzalez, C.; Schlegel, H. B.; McDouall, J. J. W. *J. Am. Chem. Soc.* **1991**, *113*, 6001. (b) Bach, R. D.; Andres, J. L.; Owensby, A. L.; Schlegel, H. B.; McDouall, J. J. W. *J. Am. Chem. Soc.* **1992**, *1147*, 7207. (c) Bach, R. D.; Owensby, A.; Andres, J. L.; Schlegel, H. B. *J. Am. Chem. Soc.* **1991**, *113*, 7031.

Table 2. MP2/6-31G* SCRF Relative Energies for Peroxyformic Acid Transition States, Reactant Clusters, and Reactants (Energies in kcal/mol)

	dipole moment[a] (debye)	MP2/6-31G* [b] (gas phase)	method I[c] $\epsilon = 4.8$	MP2/6-31G* $\epsilon = 32.7$	method II[d] $\epsilon = 4.8$	MP2/6-31G* $\epsilon = 32.7$
1 (C_2H_4)	1.23	−4.30[e]	−4.09[e]	−4.00[e]	−3.12[e]	
TS-2	3.24	16.46[f]	16.47[f]	16.06[f]	15.21[f]	15.25[f]
3 (H_2S)	1.61	−3.85	−3.37	−3.19	−2.37	−2.03
TS-4	7.45	24.87	19.96	17.30	13.60	
5 (H_2SO)	3.60	−4.71	−6.03	−5.43	−3.51	
TS-6	2.47	13.41	15.40	16.17	14.15	14.23
7 (Me_2S)	1.76	−8.40	−5.33	−5.15		
TS-8	6.45	7.99	5.60	4.34	3.54	
9b (Me_2SO)	4.26	−7.67	−8.76	−8.38		
TS-10	4.57	7.84	8.61	8.80	10.33	
11 (NH_3)	2.52	−10.66	−10.22	−10.08		
TS-12	7.78	21.48	14.73	11.52	7.89	5.70
13 (PH_3)	1.60	−3.93	−3.70	−3.62	−2.58	−2.30
TS-14	2.74	9.35	9.04	8.83	8.03	7.93
15 (Me_3N)	1.63	−18.35	−12.59	−12.53		
TS-16	5.09	4.25	2.37	1.46	0.01	
17 (Me_3P)	2.55	−7.07	−7.00	−6.92		
TS-18	2.05	0.65	0.72	0.72	1.85	
reactants[g]						
HCO_3H	1.62		−0.34[g]	−0.47[g]	−5.62[g]	−6.46[g]
C_2H_4	0.00		0.00	0.00	−1.12	−1.20
H_2S	1.40		−0.44	−0.60	−2.86	−3.29
H_2SO	4.11		−2.38	−3.28	−9.00	−10.14
Me_2S	1.76		−0.37	−0.50	−2.93	
Me_2SO	4.62		−1.84	−2.53	−9.86	
NH_3	1.97		−1.03	−1.38	−5.46	−6.07
PH_3	0.84		−0.18	−0.24	−1.24	−1.10
Me_3N	0.84		−0.06	−0.08	−2.16	
Me_3P (fc)	1.34		−0.18	−1.46	−2.48	

[a] Dipole moment of the MP2/6-31G* geometry. [b] Gas-phase activation barriers and cluster stabilizatino energies without ZPE correction. [c] The Frisch/Wiberg model using the Onsager reaction fierld with a spherical cavity. [d] The Tomasi approximation with overlapping spheres. [e] Reactant cluster stabilization energies relative to isolated reactants. [f] Transition state activation barriers relative to isolated reactants. [g] Stabilization energies of the reactants in the various solvent model systems.

energy surfaces involving O−O bond breaking can be traced to the total inadequacy of Hartree−Fock (HF) theory to describe oxygen atom transfer from a peroxide. For example, the bond dissociation energy (BDE) of peroxyformic acid into a hydroxyl radical and a formyloxyl radical ($HCO_2H \rightarrow HCO_2^{\bullet} + HO^{\bullet}$) is computed to be 1.0 kcal/mol at the HF/6-31G* level of theory. Consequently, there are no energetic consequences of breaking an O−O bond on the HF potential energy surface. When dynamic electron correlation correction is included, the BDE of HCO_3H is 50.7 kcal/mol at the MP4//MP2/6-31G* level.[13]

Oxidation of Ethylene. We elected to include ethylene in this series of nucleophiles since the carbon−carbon double bond is weakly nucleophilic and considerable experimental data on the formation of epoxides from alkenes are available.[16] The rate of alkene epoxidation has been shown to be a function of the concentration of the peroxy acid.[16a] When the peroxy acid is present in high concentration a dimer can form and upon dilution with additional solvent the activation energy for the oxidation of propene was lowered and an increase in entropy of activation was observed. The stabilization energy for dimeric peroxyformic acid with respect to isolated reactants was computed to be 7.5 kcal/mol, respectively.[15] This dimer utilizes both of its relatively acidic hydrogens ($pK_a = 7.1$) in hydrogen bonding and is a situation consistent with bonding interactions observed in the solid state.[17] The stabilization energy for reactant cluster **1** derived from complexation of peroxyformic acid with ethylene is 3.98 kcal/mol (Figure 1). These data are therefore consistent with experiment[16a] in that a dilution of the peroxy acid concentration would diminish the concentration of the dimer and hence increase the concentration of reactant complex **1** (eq 1). This would result in an increase in the observed rate for this bimolecular epoxidation reaction. The classical activation barrier for conversion of reactant complex **1** to its oxirane is predicted to be 20.2 kcal/mol. It is noteworthy

$$[HCO_3H]^2 + CH_2{=}CH_2 \underset{k_{-1}}{\overset{k_1}{\rightleftharpoons}} HCO_3H + \mathbf{1} \xrightarrow{k_2} \mathbf{TS\text{-}2} \longrightarrow \underset{CH_2-CH_2}{\overset{O}{\triangle}} + HCO_2H \quad (1)$$

(13) At the QCISD(T)//QCISD/6-31G* level the predicted D_e for HCO_3H is 50.0 kcal/mol when the contributions of triple excitations are included. A scan of the potential energy for O−O bond elongation in hydrogen peroxide (HO−OH), water oxide (H_2O−O), and peroxyformic acid (HCO_2−OH) has shown that calculations at the MP4SDTQ/6-31G*//MP2/6-31G* level yield geometries and energetics sufficiently reliable for mechanistic studies of oxygen atom transfer.[15a] The O−O bond dissociation energies for H_2O_2 and CH_3CO_3H at the G2 (MP2) level[14a] of theory are $D_0 = 49.87$ and 48.49 kcal/mol.[14b]

(14) (a) Curtiss, L. A.; Raghavachari, K.; Pople, J. A. *J. Chem. Phys.* **1993**, *98*, 1293. (b) Bach, R. D. Unpublished results.

(15) (a) Bach, R. D.; Andres, J. L.; Gonzalez, C.; Fox, G. L.; Estevez, C. M.; Winter, J. E.; Schlegel, H. B.; McDouall, J. J. W. *J. Am. Chem. Soc.* Submitted for publication. (b) Unpublished results.

(16) (a) Dryuk, V. G. *Russ. Chem. Rev.* **1985**, *54*, 986. (b) Valov, P. I.; Blyumberg, E. A.; Filippova, T. V. *Kinet. Katal.* **1967**, *8*, 760. (c) Swern, D. *Organic Peroxides*; Wiley Interscience: New York, **1971**; Vol. II, pp 73−74. (d) Swern, D. *J. Am. Chem. Soc.* **1947**, *69*, 1692. (e) Lynch, B. M.; Pausacker, K. H. *J. Chem. Soc.* **1955**, 1525. (f) Hanzlik, R. P.; Shearer, G. O. *J. Am. Chem. Soc.* **1975**, *106*, 1401.

(17) For a discussion of intermolecular hydrogen bonding in the crystal structure of a peroxy acid, see: Belitskus, D.; Jeffrey, G. A. *Acta Crystallogr.* **1965**, *18*, 458.

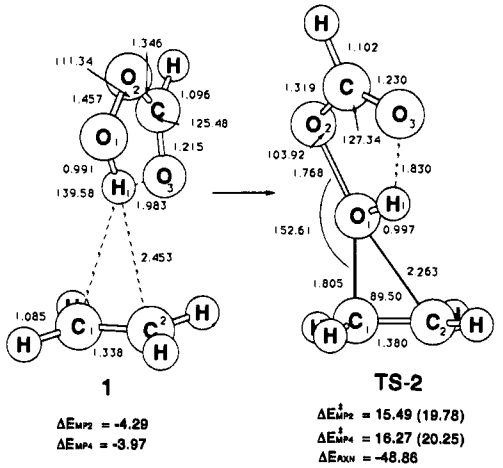

Figure 1. Reactant cluster and transition state for the epoxidation of ethylene by peroxyformic acid. Geometries at MP2/6-31G*, reactant cluster **1** constrained to C_s symmetry. Relative energies at MP2/6-31G* (with ZPE) and MP4/6-31G*//MP2/6-31G* levels, in kcal/mol. Activation barrier relative to reactant cluster given in parentheses. Distances in Å and angles in deg.

that the intramolecular hydrogen bond in peroxyformic acid is not disrupted in complex **1**. We predict on the basis of calculations at the MP4//MP2/6-31G* level that **TS-2** is 16.3 kcal/mol (with ZPE) higher in energy than its isolated reactants (Figure 1). In a spiro orientation of the peroxy acid the O−O−C−O plane is at right angles ($\theta = 90°$) to the C=C bond of the alkene. At the MP2 level the peroxy acid approaches the π-bond of ethylene in an approximate spiro manner ($\theta = 60°$), and the electrophilic oxygen atom in **TS-2** is directly over one carbon atom. Since the energy difference between the symmetrical[5] and unsymmetrical (**TS-2**) transition states is so small (~0.2 kcal/mol) the potential energy surface for approach of the electrophile must be extremely shallow. Consequently, the two-electron stabilization interaction between the oxygen lone pair and the π^* orbital of ethylene that requires a symmetrical TS must also be negligible. The mechanism for oxygen atom transfer entails an S_N2 like back-side attack of the nucleophilic π-bond of ethylene on the O−O bond. The O−O bond is 21.3% elongated in **TS-2** relative to **1** and the O−O−C bond angle has contracted 7.4° to move the carbonyl oxygen atom 0.15 Å closer to the migrating hydrogen. As noted previously,[5] the hydrogen migration takes place *after the barrier is crossed.* However, the transition vector at the saddle point is dominated by the 1,4-migration of the lighter hydrogen atom. In a related study we have predicted the barriers (MP4//MP2/6-31G*) for peroxyformic acid epoxidation of ethylene, 2-butene, isobutylene, 1,3-butadiene, and acrylonitrile to be 16.3, 10.4, 10.6, 12.4, and 17.1 kcal/mol, respectively.[15a] Both the magnitude of the barriers and the reactivity trends for alkene epoxidation are in excellent agreement with experiment.[16] The high negative entropy ($\Delta S^{\ddagger} = -38.29$ cal/(mol deg)) for **TS-2** is also consistent with experiment. The overall oxygen atom transfer reaction yielding formic acid and ethylene oxide is exothermic by 48.86 kcal/mol.

A Hartree−Fock stability analysis of the ethylene and peroxyformic acid transition state (MP2/6-31G* geometry) shows an RHF → UHF instability (root = −0.110 au). Optimization of the SCF wave function at the UHF level yields an energy lowering of 23.3 kcal mol^{-1} relative to the RHF solution. A spin-unrestricted MP4 calculation including spin-annihilation up to $S + 4$ (PMP4) gives a barrier of 18.9 kcal mol^{-1}. This suggests that when an instability of this magnitude exists in the reference wave function, a more reliable barrier will be obtained by reoptimizing the wave function at the UHF level and performing a PMP4 calculation to obtain the barrier. This transition state has a greater wave function instability than the others included in this study (Table 1).[18]

Oxygen atom transfer to ethylene proceeds in a nearly ideal spiro fashion at the QCISD, CCSD, and CCSD(T) level (6-31G*).[15a] A symmetrical approach was also observed for the epoxidation of propene with HCO_3H at the QCISD/6-31G* level. The magnitudes of the classical activation epoxidation barriers of 16.3, 18.9, and 18.8 kcal/mol at MP4//MP2/6-31G*, PMP4//MP2/6-31G*, and QCISD(T)//QCISD/6-31G* are quite comparable. Consequently, the remainder of this study utilizes the MP4(SDTQ)//MP2/6-31G* level of theory.

Oxidation of Sulfides and Sulfoxides. One of the current mechanistic questions relevant to this study is the relative nucleophilicity of a sulfide versus its sulfoxide and the use of these functional groups to assess the electronic nature of oxygen-transfer reagents.[19] In these studies it was recognized that the preferential complexation of the oxidizing agent with either the sulfur or sulfoxide moiety could alter the chemoselectivity of competitive oxidation. The oxidation of sulfides shows no clear dependence of rates on solvent dielectric constant but rather upon specific interactions between solvent and solute.[4] Under typical laboratory conditions the oxidation of a sulfide can be stopped readily at the sulfoxide stage if desired (eq 2) and its sulfone is not formed unless additional oxidizing agent is added or more vigorous reaction conditions are introduced. Consequently, a sulfide has been considered historically to be much more nucleophilic than its sulfoxide. However, rate ratios (k_1/k_2) for sulfide versus sulfoxide oxidation as low as 3 and as high as 900 have been observed. This rate ratio is of considerable importance to the synthetic chemist if a high chemoselectivity in the oxidation of a sulfide is desired. The highest rate ratios were observed in more acidic solvents where the more basic sulfoxide can be highly solvated thus lowering its ground state energy.

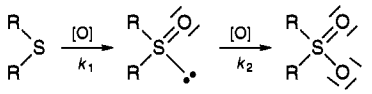

(2)

Kinetic studies have suggested a mechanism for oxidation involving nucleophilic attack by the sulfide on the intramolecularly hydrogen-bonded form of the peroxy acid as depicted in **TS-A** (eq 3).

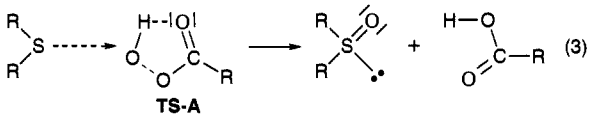

(3)

The mechanisms of alkene and sulfide oxidation have many similarities. The oxidation of cyclohexene and *p*-nitrodiphenyl sulfide by peroxybenzoic acid in benzene solvent has enthalpies of activation of 8.7 and 11.0 kcal/mol, respectively.[4b] The entropies of activation are also large and negative for both reactions (−29 and −24 cal/(deg mol)).

The computational expenses incurred when dealing with relatively large systems often mandate the omission of substituents on the substrates that are studied. Consequently we

(18) The CASSCF occupation numbers of HOMO and LUMO for a calculation involving 10 electrons and 10 orbitals are 1.90 and 0.15, respectively,[15a] indicating a relatively strong orbital interaction which leads to the RHF → UHF instability.

(19) (a) Adam, W.; Hase, W.; Lohray, B. B. *J. Am. Chem. Soc.* **1991**, *113*, 6202. (b) Ballistreri, F. P.; Tomaselli, G. A.; Toscano, R. M.; Conte, V.; DiFuria, F. *J. Am. Chem. Soc.* **1991**, *113*, 6209.

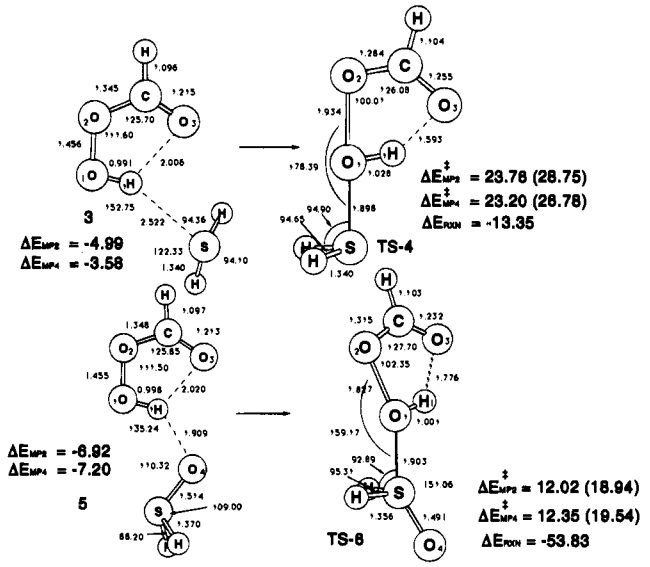

Figure 2. Reactant clusters and transition states for the oxidation of hydrogen sulfide and hydrogen sulfoxide by peroxyformic acid. Geometries at MP2/6-31G*. Relative energies at MP2/6-31G* (with ZPE) and MP4/6-31G*//MP2/6-31G* levels, in kcal/mol. Activation barriers relative to reactant clusters given in parentheses. Distances in Å and angles in deg.

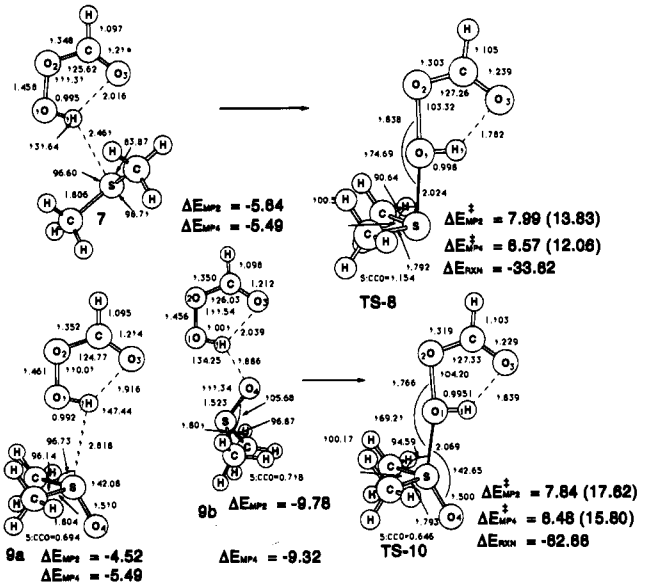

Figure 3. Reactant clusters and transition states for the oxidation of dimethyl sulfide and dimethyl sulfoxide by peroxyformic acid. Geometries at MP2/6-31G*. Relative energies at MP2/6-31G* (with ZPE) and MP4/6-31G*//MP 2/6-31G*, in kcal/mol. Activation barriers relative to reactant clusters in parentheses. Distance-to-plane (a:xyz) measures the perpendicular distance from atom a to the plane formed by atoms x, y, and z. Distances in Å and angles in deg.

initiated this mechanistic investigation of the relative rates of sulfide versus sulfoxide oxidation using H_2S and H_2SO. Reactant clusters for H_2S and H_2SO (**3** and **5**) with peroxyformic acid were stabilized by 3.6 and 7.2 kcal/mol (Figure 2) relative to isolated reactants. We were immediately struck by the fact that the classical activation barrier for the oxidation of H_2S ($\Delta E^{\ddagger}$ = 26.8 kcal/mol, **TS-4**) was significantly higher than that for the epoxidation of ethylene (20.2 kcal/mol). The $\Delta\Delta E^{\ddagger}$ was approximately the same when measured from either isolated reactants or a reactant complex. We were further disturbed to observe that H_2SO was considerably more reactive toward peroxyformic acid than H_2S ($\Delta\Delta E^{\ddagger}$ = 7.2 kcal/mol). Although this reactivity trend was improved when a solvation correction was introduced with a self-consistent reaction field (SCRF) calculation, the $\Delta\Delta E^{\ddagger}$ was <1 kcal/mol using the Tomasi SCRF method (Table 2).[5] Using the less rigorous methods of Onsager the incorrect reactivity trend still prevails and the sulfoxide is predicted to have a lower activation barrier than the sulfide (Table 2). However, one should not lose sight of the fact that this could indeed be the correct order of reactivity for nucleophiles bearing only hydrogen substituents.

The above rather disturbing trends are not in accord with experimental data for alkyl- or aryl-substituted sulfides and sulfoxides. Since our epoxidation studies at this level of theory on a series of substituted alkenes[15a] were in good agreement with condensed phase experimental data,[16c] it seemed prudent to examine reactivity trends for oxidation at sulfur bearing alkyl substituents. Basically the same relative behavior noted for the formation of gas-phase reactant clusters was observed with and without methyl substituents. The computed stabilization energies for the hydrogen-bonded complex of peroxyformic acid with dimethyl sulfide (DMS) and dimethyl sulfoxide (DMSO) are 5.5 and 9.3 kcal/mol, respectively (Figure 3). Of particular interest from an historical perspective is that the predicted gas-phase nucleophilicities of DMS (**7**) and DMSO (**9b**) at this level of theory are now predicted to be virtually identical. The classical barriers for the oxidation of DMS (**TS-8**) and DMSO (**TS-10**) are 6.6 and 6.5 kcal/mol when measured from isolated reactants. Activation barriers of 12.1 and 15.8 kcal/mol are predicted relative to gas-phase clusters **7** and **9b** reflecting the greater basicity of the sulfoxide oxygen atom. The proton affinity (Table 3) of DMSO is 22.0 kcal/mol higher than that of DMS. The proton affinity of the oxygen atom in DMSO is 37.4 kcal/mol greater than that of its sulfur atom. Consequently, complexation of the sulfoxide oxygen atom with the peroxy acid (**9b**) stabilizes the reactant cluster by 3.8 kcal/mol more than complexation with the sulfur atom (**9a**, Figure 5). The $S-O_1-O_2$ bond angle of 175° in **TS-8** is consistent with an S_N2 attack by the higher lying of the two sulfur lone pairs of electrons on the O−O bond of the peroxy acid. The O−O bond in **TS-8** is elongated by 26% while the S−O bond in DMSO is 75% developed. The transition state for DMSO oxidation (**TS-10**) comes somewhat earlier along the reaction path as reflected in a shorter (0.072 Å) O−O bond and a much greater exothermicity ($\Delta\Delta E$ = 29.1 kcal/mol).

Since the gas-phase reactivities (GPR) of DMS and DMSO are comparable, the observed chemoselectivity for sulfide oxidation must be a consequence of solvent interactions in the condensed phase. The increase in dipole moment (Table 3) in the transition state for oxygen atom transfer from peroxyformic acid to DMS (**TS-8**) is rather large since a highly polarized S−O bond is being formed. The calculated dipole moment of DMS is 1.76 D while that of **TS-8** is 6.45 D. Thus an increase in solvent polarity should stabilize the transition state (**TS-8**) for sulfide oxidation. Contrariwise, a very small increase in dipole moment (0.31 D) is predicted upon going to the transition state for the oxidation of DMSO to dimethyl sulfone (**TS-10**). Both the dipole moment and basicity of DMSO are greater than those of DMS. Therefore, an increase in solvent polarity *and* the acidity of the solvent should stabilize the ground state of DMSO much more than its transition state for oxidation (**TS-10**). This should be particularly true if a protic solvent was used. Indeed, the role of solvent polarity versus solvent acidity and the effects of such specific molecular interactions on the relative nucleophilicity of a sulfide versus a sulfoxide were clearly understood by Edwards and his co-workers.[4] These trends are now presented in a more quantitative way in Figure 4 where it is shown, based upon a comparison with SCRF calculations, that

Table 3. A Comparison of Transition State Parameters for the Oxidation of a Series of Nucleophiles by Peroxyformic Acid[d]

	H_2S	NH_3	C_2H_4	H_2SO	PH_3	Me_2S	Me_2SO	Me_3N	Me_3P
$\Delta E^{\ddagger}$ (from isolated reactants)	23.20	18.35	16.27	12.35	9.47	6.57	6.48	0.94	0.54
$\Delta E^{\ddagger}$ (from reactant cluster)	26.78	28.45	20.25	19.54	13.11	12.06	15.80	13.01	7.54
ΔE_{RXN} ($E_{reactants} - E_{products}$)	−13.35	+7.76	−48.86	−53.63	−63.13	−33.62	−62.68	+3.08	−87.64
ΔE_{RXN} (Nuc + $^1O \rightarrow$ Nuc−O)[a]	−107.88	−86.76	−143.38	−148.15	−157.66	−128.14	−157.20	−91.44	−182.17
ΔE (stabilization of reactant cluster)	−3.58	−10.10	−3.98	−7.20	−3.64	−5.49	−9.32	−12.07	−7.00
ΔS (of reactant cluster)	−23.36	−30.05	−26.10	−27.92	−22.27	−30.75	−25.58	−36.62	−36.80
proton affinity of nucleophile (kcal/mol)	174.0	218.0	168.6	205.7[b]	193.6	199.9	221.9[b]	225.1	232.2
fractions of electrons transferred to peracid in TS	0.65	0.67	0.42	0.44	0.35	0.56	0.39	0.51	0.13
$\Delta S^{\ddagger}$ (from isolated reactants)	−38.60	−33.88	−38.29	−39.34	−36.36	−37.99	−44.77	−35.20	−43.19
$\Delta S^{\ddagger}$ (from reactant cluster)	−15.24	−3.83	−12.19	−11.42	−14.09	−7.23	−19.19	1.43	−6.39
$\Delta H^{\ddagger}$ (from isolated reactants)	22.90	19.30	16.54	13.06	9.14	6.83	4.96	1.26	−0.64
$\Delta G^{\ddagger}$ (from isolated reactants)[c]	34.40	29.41	27.96	24.79	19.99	18.15	18.31	11.75	12.24
$\Delta G^{\ddagger}$ (from reactant cluster)[c]	29.67	29.55	22.86	22.95	15.66	13.85	19.42	12.86	8.39

[a] The MP4/6-31G* energy for ^1O is −74.79315. [b] The proton affinities for the sulfur atoms in H_2SO and Me_2SO are 158.0 and 184.5 kcal/mol, respectively. [c] Enthalpies, entropies, and free energies calculated at 298 K. [d] Relative energies from the MP4/6-31G*//MP2/6-31G* energy. Thermodyanmic data from the MP2 frequency calculations, using the 6-31G* basis set for the hydrogen-substituted nucleophiles and the 3-21G basis set for the methyl-substituted nucleophiles. Entropies in eu and energies in kcal/mol.

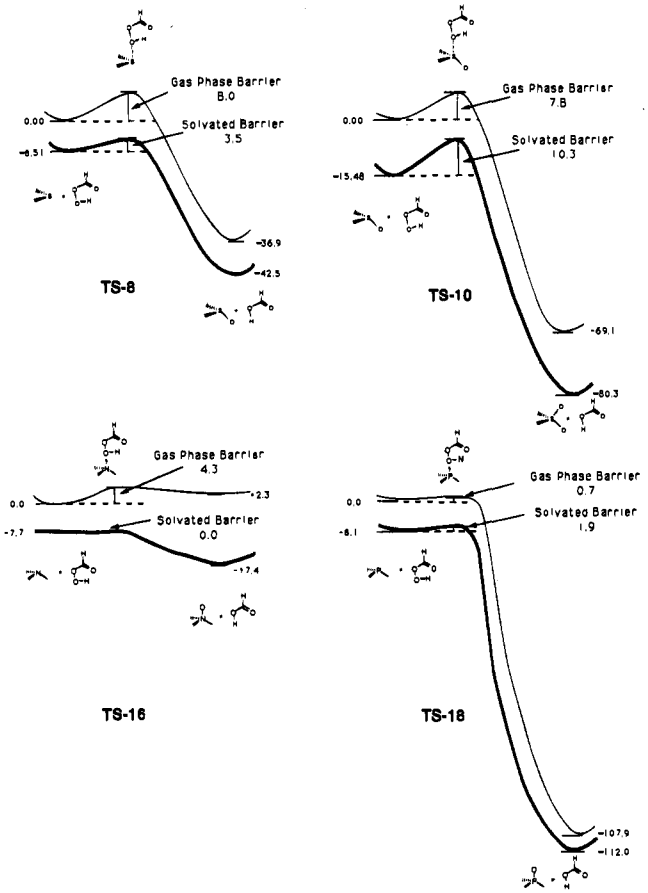

Figure 4. Relative energies for the isolated reactants, transition states, and products for the oxidation of dimethyl sulfide (**TS-8**), dimethyl sulfoxide (**TS-10**), trimethylamine (**TS-16**), and trimethylphosphine (**TS-18**) by peroxyformic acid at MP2/6-31G*, without ZPE. The bold-faced line represents the effect of a solvent with a dielectric constant of 4.806 using the Tomasi SCRF model at MP2. Energies in kcal/mol.

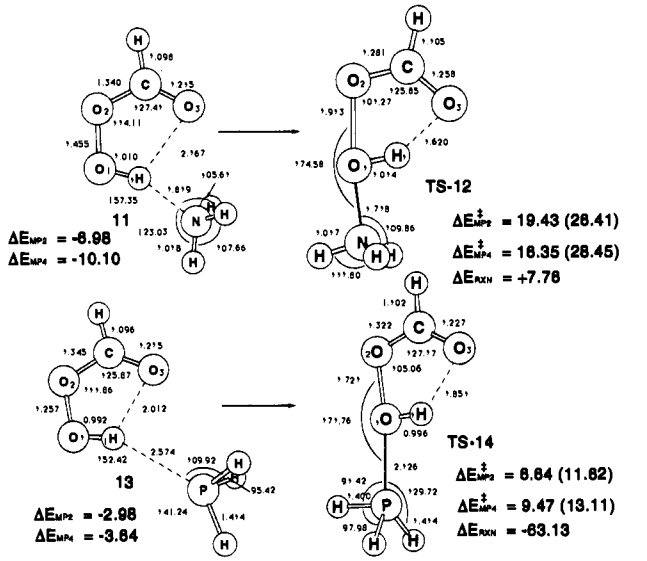

Figure 5. Reactant clusters and transition states for the oxidation of ammonia and phosphine by peroxyformic acid. Geometries at MP2/6-31G*. Relative energies at MP2/6-31G* (with ZPE) and MP4/6-31G*//MP2/6-31G* levels, in kcal/mol. Activation barriers relative to reactant clusters in parentheses. Distances in Å and angles in deg.

the solvated TS for sulfide oxidation is decreased from 8.0 to 3.5 kcal/mol upon going from the gas to the condensed phase. Because of the greater stabilization of the ground state (−15.48 kcal/mol), the activation energy for sulfone formation is higher (10.3 kcal/mol) in the condensed phase than it is in the gas phase (7.8 kcal/mol). Another factor that could conspire to lower the activation energy for sulfoxide oxidation is its relatively high exothermicity. The ΔE for **TS-10** is 37.8 kcal/mol higher than that for **TS-8** (Figure 4) despite the fact that we have used a relatively low dielectric constant of 4.8. Although a much earlier TS should be predicted for sulfoxide versus sulfide oxidation, the latter barrier is still higher when solvation is treated explicitly. Hence, any discussion of the nucleophilicity of a sulfide versus its sulfoxide must take into consideration those factors that influence its gas-phase reactivity (GPR) relative to its condensed-phase reactivity (CPR).

Oxidation of Amines and Phosphines. Two basic reactivity trends that are firmly ensconced in organic mechanistic lore concerning amines and phosphines are that the former are more basic while the latter more polarizable third row element is much more nucleophilic. Our calculations on the peroxy acid oxidation of NH_3 and PH_3 are indeed consistent with this conventional wisdom. The potential energy well for the complexation of NH_3 (**11**) is 10.1 kcal/mol below isolated reactants while that for PH_3 has a lesser $\Delta E_{stab} = -3.6$ kcal/mol (Figure 5). The classical activation barriers for the formation of H_3P-O are lower than those for H_3N-O formation when computed either from isolated reactants or from gas-phase clusters **11** and **13** ($\Delta E^{\ddagger} = 28.4$ and 13.1 kcal/mol). However, when an SCRF correction is made employing the Tomasi method (Table 2) the relative reactivities based upon activation barriers for NH_3 and PH_3 oxidation are virtually identical (7.89 and 8.03 kcal/mol, respectively).

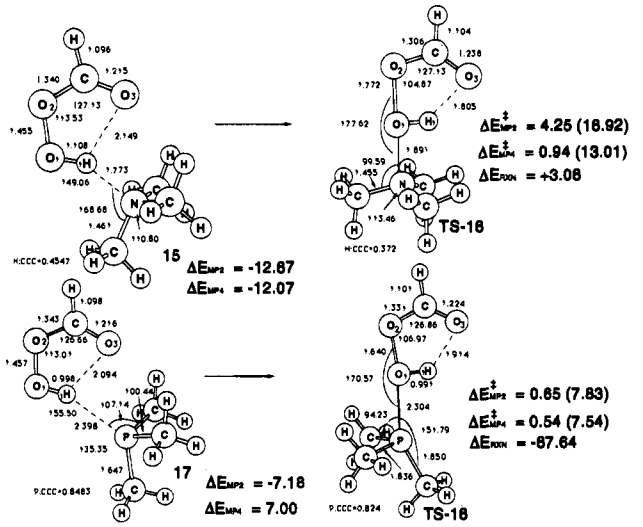

Figure 6. Reactant clusters and transition states for the oxidation of trimethylamine and trimethylphosphine by peroxyformic acid. Geometries at MP2/6-31G*. Relative energies at MP2/6-31G* (with ZPE) and MP4/6-31G*//MP2/6-31G*, in kcal/mol. Activation barriers relative to reactant clusters in parentheses. Distance-to-plane (a:xyz) measures the perpendicular distance from atom **a** to the plane formed by atoms x, y, and z. Distances in Å and angles in deg.

The above lessons on the essential role of alkyl groups in examining gas-phase reactivity versus condensed-phase reactivity prompted the use of trimethylamine and trimethylphosphine as nucleophiles despite the rather large number of basis functions involved for the TS at the 6-31G* level (142 and 146). The difference in the energies of the stabilization of peroxyformic acid with $N(CH_3)_3$ and $P(CH_3)_3$ (5.1 kcal/mol) is quite comparable to the differences in their proton affinities (7.1 kcal/mol, Table 3) reflecting the greater basicity of the amine. In general the predicted ΔE_{stab} for reactant clusters paralleled the proton affinities (Table 3). The intrinsic nucleophilicity of these two Lewis bases when measured relative to isolated reactants did come as a surprise. The classic activation barriers for amine versus phosphine oxidation are 0.94 and −0.62 kcal/mol, respectively, when measured relative to isolated reactants. A predicted $\Delta\Delta E^{\ddagger}$ for **TS-16** and **TS-18** (Figure 6) of only 0.4 kcal/mol again suggests that the polarizability of third-row elements plays only a minor role in their ability to function as nucleophiles. When the barriers are computed relative to gas-phase clusters, the relative gas-phase reactivity is closer to that which would be anticipated ($\Delta\Delta E^{\ddagger} = 5.5$ kcal/mol) based upon the relative depth of the potential energy well for cluster formation (i.e. basicity). However, their relative reactivity toward electrophilic oxygen based upon a Tomasi SCRF correction at a relatively low dielectric constant ($\epsilon = 4.8$) is comparable to that computed relative to their gas-phase clusters except we now predict a slightly higher barrier (1.85 kcal/mol) for phosphine oxidation. We observed no effect of solvation on the activation barrier for amine oxidation despite the fact that the dipole moment for amine oxidation increases on going from the ground to the transition state. A slight reduction in dipole moment is predicted for trimethylphosphine oxidation (Table 2). The increase in dipole moment for amine oxidation is reflected in a change from endo- to exothermicity (Figure 4). While the k_1/k_2 rate ratio for sulfide/sulfoxide reactivity was influenced markedly by a solvation correction, no such effect is noted for amine versus phosphine reactivity. The most obvious difference in the potential energy surfaces for these two oxidations is in the overall energy (ΔE) or enthalpy of reaction (Table 3). While the formation of $(CH_3)_3N{-}O$ is slightly endothermic ($\Delta E = +3.1$ kcal/mol), the formation of the much stronger P−O bond in **TS-18** is highly exothermic by 87.6 kcal/mol. In an effort to estimate the strength of the bond being formed between the nucleophile (:NUC) and oxygen, the energy differences between O−NUC and :NUC plus a singlet oxygen atom (^1O) were computed (Table 3). No correlation between these values and the bond energy or $\Delta E^{\ddagger}$ of reaction is in evidence.

The $\Delta G^{\ddagger}$ (298 K) of oxidation of $(CH_3)_3N$ and $(CH_3)_3P$ are relatively close (11.7 and 12.2 kcal/mol) when measured relative to isolated reactants. However, the gas-phase $\Delta G^{\ddagger}$ for the former increases to 12.9 kcal/mol and the latter decreases to 8.4 kcal/mol when $\Delta G^{\ddagger}$ is computed relative to their entropically constrained reactant clusters. This $\Delta\Delta G^{\ddagger}$ (4.5 kcal/mol) is largely due to the relatively high negative entropy of activation for $(CH_3)_3P$ oxidation (−44.8 versus −35.2 kcal/mol, Table 3). In general, the entropies of activation were in good accord with experiment when calculated relative to isolated reactants. As anticipated, the change in entropy was much smaller when measured relative to the reactant clusters. The entropy differences do not appear to be a function of steric crowding due to the methyl groups when the nucleophilic trivalent central atom N or P becomes tetrahedral in the oxidation product. When the distance of the central atom above the plane defined by the three carbon atoms directly attached to it is measured (a:xyz, Figure 6) the pyramidality of the molecule changes surprisingly little upon going from reactant to product. This also suggests that "back strain" due to compression of the alkyl groups in the TS should have little influence upon the activation barrier for oxidation. Thus, we attribute the higher GPR of a weakly basic phosphine to entropy effects and to a very early transition state. Consistent with this suggestion the P−O and N−O bonds in **TS-18** and **TS-16** are 2.30 and 1.89 Å, respectively. It now remains to compare these gas-phase data with experiments in the condensed phase.

SCRF Calculations. Solvation effects may be estimated using molecular dynamics simulations in which the solvent molecules are included explicitly or by the continuum models which consider the solvent as an infinite dielectric continuum. This self-consistent reaction field (SCRF) method models the interaction of the dipole of the solute with the polarizable solvent. An extension of this model up to angular momentum $l = 7$ for the solute charge distribution and the use of an ellipsoidal cavity has been developed by Rivail and co-workers.[10c] These models do not take into account local solvent−solute interactions. An improved model has recently been developed by Tomasi and co-workers[10a] which involves the use of more realistic shapes for the solute cavity and a more accurate representation of the solute charge distribution. The method involves the generation of a cavity from spheres centered at each atom in the molecule and the calculation of point charges on the cavity surface which mimic the reaction field. The magnitude of these charges is proportional to the derivative of the solute electrostatic potential at each surface point. The point charges are then included in the one-electron Hamiltonian which induces polarization of the solute. This process is repeated until the surface charges are self consistently equilibrated in the solute charge distribution; this method is called the polarizable continuum model (PCM). For the PCM model the sphere radii assigned to each atom are dependent on the atom type and basis set. Suitable parameters have been developed by Aguilar and Olivares del Valle which yield the atomic radii as linear functions of the Mulliken charges for various basis sets.[10b]

Our initial efforts were directed at examining the effect of solvent at the HF/6-31G* level as predicted by the multipole SCRF method of Rivail and co-workers. We considered four solvents (chloroform, $\epsilon = 4.8$; dichloromethane, $\epsilon = 9.08$;

methanol, $\epsilon = 32.7$; acetonitrile, $\epsilon = 38.0$) of varying dielectric constant for the parent (bearing only hydrogen substituents) substrates. For the cases of dimethyl sulfide, dimethyl sulfoxide, and trimethylamines we performed calculations with only chloroform and methanol solvents. For the reactions of ethylene, hydrogen sulfoxide, and phosphine the effect of solvation is predicted to be negligible. In the case of hydrogen sulfide and ammonia, the transition states formed with peroxyformic acid undergo a substantial stabilization relative to reactants yielding a significant decrease in activation barriers relative to the gas phase. Of particular interest is the trend predicted for hydrogen sulfide and sulfoxide reactions. In the gas phase the sulfoxide barrier is approximately half that of the sulfide reaction. When the effect of solvent is included the sulfoxide transition state undergoes a minimal stabilization, whereas the sulfide transition state shows a dramatic stabilization. In the most polar solvent we have considered (acetonitrile), the barriers for these two reactions are predicted to be essentially the same. The trends predicted at the Hartree−Fock level appeared to be inconsistent with experimental data in solution and are quite likely an artifact of the level of theory. Consequently, we report only SCRF data obtained at the MP2 level.

The simpler Onsager SCRF model at the MP2/6-31G* level predicts the sulfoxide reaction to be preferred by 1.1 kcal/mol. With the exception of H_2SO and $(CH_3)_2SO$, an increase in the dielectric constant of the solvent from 4.8 to 32.7 resulted in a decrease in activation energy (Table 2).

The Tomasi model which allows for a more realistic shape of the solute cavity and local solute−solvent charge interactions predicts inversion of the gas-phase barriers such that the sulfide oxidation is preferred, in excellent agreement with experiment. Only the sulfoxide barriers were higher in the SCRF model than in the gas phase. An increase in solvent dielectric constant from 4.8 to 32.7 had only a modest effect upon the predicted barrier heights (Table 2).

Since the attacking atom in this reaction is a highly electronegative oxygen atom, the energetics of the developing O−NUC bond is also a major consideration when determining relative reactivity of this series of nucleophiles (:NUC). In protic solvents nucleophilicity and basicity are not parallel. Experimentally[4] it has been noted that in the nonpolar solvent dioxane ($\epsilon = 2.2$) the rate of oxidation of a sulfide is only a factor of 3.3 larger than the rate of oxidation of the analogous sulfoxide. In the protic solvent 2-propanol the activation energies are such as to indicate that a rate inversion may occur at lower temperatures. However, in trifluoroethanol k_s/k_{so} can be as high as 900. The specific hydrogen-bonding and proton-transfer reactions are the dominant factors in determining relative "nucleophilicity". Moreover, upon closer inspection we must realize that our predilection to assign phosphorus a much greater nucleophilic capacity than nitrogen or sulfur is based upon nucleophilic constants that were determined in a protic solvent.[1] In methanol solvent nucleophilic constants show an order of reactivity toward methyl iodide where $R_3P > R_3N > R_2S$ and their relative rates are 2512:25:1. In the present study we predict a trend for GPR of $R_3P \sim R_3N > R_2S \sim R_2SO \gg CH_2{=}CH_2$. The CPR for this series of nucleophiles based upon SCRF data for a relatively nonpolar solvent suggest a trend more consistent with the experimental data.[16] The effects of hydrogen bonding to the nucleophile play a dominant role in the interactions with reactivity of nucleophiles in general. Similar effects have been noted for charged nucleophiles. For example, reactivity differences between the halides are markedly diminished in protic solvents.[1]

Summary

Perhaps the most significant finding of this study pertains to the origin of the observed reactivity of this series of nucleophiles. The activation barrier for alkene epoxidation is greater than that for sulfide oxidation in accord with conventional wisdom. A sulfide has typically been described as a better nucleophile than a π-bond. However, the gas-phase intrinsic reactivity of a sulfide is virtually identical to that of a sulfoxide and the chemoselectively observed in sulfide-to-sulfoxide oxidations is a consequence of the fact that solvation lowers the transition state for sulfide oxidation and the ground state for sulfoxide oxidation. This reactivity difference is maximized in relatively acidic protic solvents where sulfoxide "nucleophilicity" is reduced as a consequence of the basicity of the sulfoxide oxygen. Both of these factors conspire to render a sulfide more "nucleophilic" than a sulfoxide. In the gas phase the free energies of activation ($\Delta G^{\ddagger}$) for the oxidation of trimethylamine and trimethylphosphine differ by only 0.5 kcal/mol when measured relative to their isolated reactants. In aprotic solvents solvation effects tend to cancel each other for amine versus phosphine oxidation, and the solvent corrected activation energies, as well as the intrinsic barriers ($\Delta E^{\ddagger}$), for these two oxidative processes are very similar in magnitude. The gas-phase classical barriers relative to a reactant cluster are more in accord with expectation and a phosphine has a greater gas-phase reactivity than an amine as a consequence of the greater basicity of the amine and a more negative entropy of activation for the phosphine. The transition state for phosphine oxidation comes early along the reaction coordinate for this highly exothermic reaction while the opposite situation prevails for endothermic amine oxide formation. The greater basicity of an amine influences both its GPR and its CPR with this difference being greatly magnified in protic solvents.

The above factors suggest to us that discussions of relative nucleophilicity are of little relevance unless a comparison between gas-phase and condensed-phase reactivity is included. In establishing mechanistic dogma concerning the order of relative nucleophilicity that is presented in standard text books[1] the effects of solvation must be emphasized. The practicing synthetic chemist desires to know which reagent reacts more rapidly under a particular set of reaction conditions. The mechanistic chemist has traditionally sought an explanation as to why.

Finally, a word of caution is in order against omission of substituents on the substrates under theoretical study. It is clear from this rather limited study that the abbreviated hydrogen-substituted nucleophiles not only gave poor results but also led to misleading mechanistic conclusions. Despite the cost in computational resources, the methyl substituents proved to be crucial to this theoretical study.

Acknowledgment. This work was supported in part by the National Science Foundation (CHE 93-06341) and a NATO Collaborative Research Grant (900707). We are also thankful to the Pittsburgh Supercomputing Center, CRAY Research, and the Ford Motor Company for generous amounts of computer time.

Supporting Information Available: Table of SCRF total energies for peroxyformic acid transition states and reactant clusters and a figure with partial geometries for reactants and oxidation products (2 pages). This material is contained in many libraries on microfiche, immediately follows this article in the microfilm version of the journal, can be ordered from the ACS, and can be downloaded from the Internet; see any current masthead page for ordering information and Internet access instructions.

JA9500973